PCCP

Accepted Manuscript

ROYAL SOCIETY OF CHEMISTRY

www.rsc.org/pccp

A Model Study on the Photochemical Isomerizations of Isothiazoles and Thiazoles

Ming-Der Su[1,2]*

[1]Department of Applied Chemistry, National Chiayi University, Chiayi 60004, Taiwan

[2]Department of Medicinal and Applied Chemistry, Kaohsiung Medical University, Kaohsiung 80708, Taiwan

*E-mail: midesu@mail.ncyu.edu.tw

Abstract

The mechanisms for photochemical isomerization reactions are studied theoretically using three model systems: 3–methylisothiazole, 4–methylisothiazole and 5–methylisothiazole. The CASSCF (ten-electron/seven-orbital active space) and MP2-CAS methods are used with the 6-311G(d) and 6-311++G(3df,3pd) basis sets, respectively. Three mechanisms: the internal cyclization–isomerization route (path A), the ring contraction–ring expansion route (path B) and the direct route (path C), are used to determine the actual photochemical reaction mechanism for these three model molecules. The structures of the conical intersections, which play a crucial role in these photo-transpositions, are determined. The intermediates and transition structures of the ground states are also calculated, to give a qualitative explanation of the reaction pathways. These model investigations suggest that the preferred reaction route is: reactant → Franck-Condon region → conical intersection → photoproduct. Particularly, the direct mechanism (path C) described in this work gives a better explanation than other pathways proposed before and is supported by the experimental observations. The results obtained allow a number of predictions to be made.

Keywords: photochemistry, photoisomerizations, photorearrangements, conical intersections, isothiazoles, thiazoles.

I. Introduction

Isothiazole and thiazole are five-membered heterocyclic molecules that are isoconjugate with the cyclopentadienyl anion and are derived from it by replacing two carbon atoms with a nitrogen atom and a sulfur atom, to give isothiazole and thiazole. The chemistry and the biological and pharmacological uses of both heterocyclic molecular systems have been reviewed extensively.[1] Commercially important isothiazoles include the artifical sweetener, saccharin, and the antibacterial sulfa drug, sulfasomizole.[2] In particular, isothiazoles have recently been studied as potential anticancer agents.[3] Sulfasomizole derivatives of isothiazole are used as antibiotics.[4] Analgesic, antipyretic, fungicidal and herbicidal activity is also reported for isothiazoles.[4.5] Thiazole is also an important parent species in the chemical industry for medicines, pesticides, dyes and photographic sensitizers and important examples of its derivatives include thiamine (vitamin B1) and the penicillines.[6] The wide biological and pharmacological applications for both isothiazole and thiazole molecules indicate that understanding their photochemistry is vital.

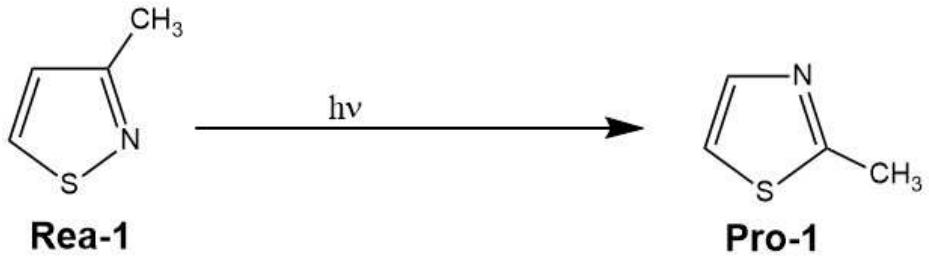

Rea-1 Pro-1 (1)

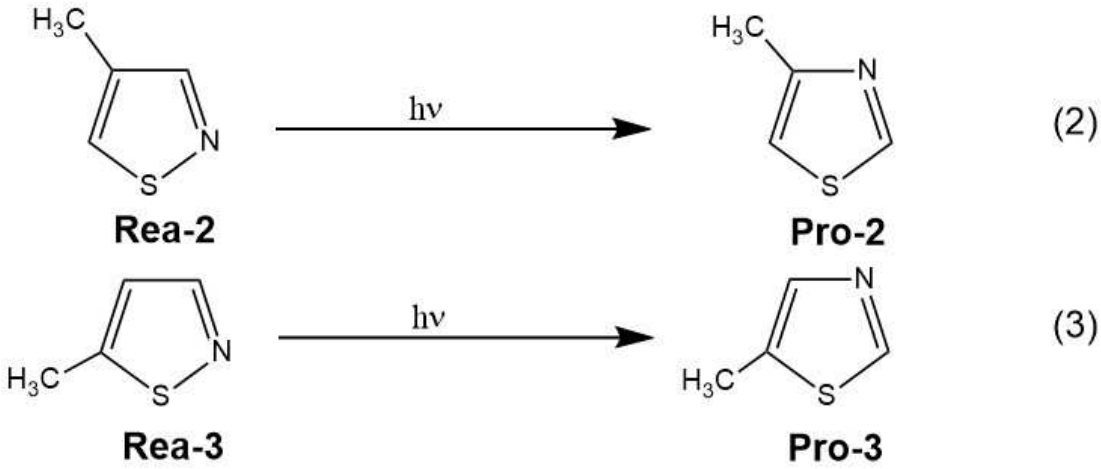

Scheme 1

The photoisomerization of isothiazole to thiazole to occurs upon photolysis in a variety of solvents.[7] Nevertheless, the reverse phototransposition of thiazole to isothiazole is reported not to occur. The studies by Pavlik and co-workers showed that methylisothiazoles undergo phototransposition to methylthiazoles in a neutral solution by a single permutation process.[8] See Scheme 1. The results of these experiments allow mechanisms to be postulated, which rationalize the experimental findings.

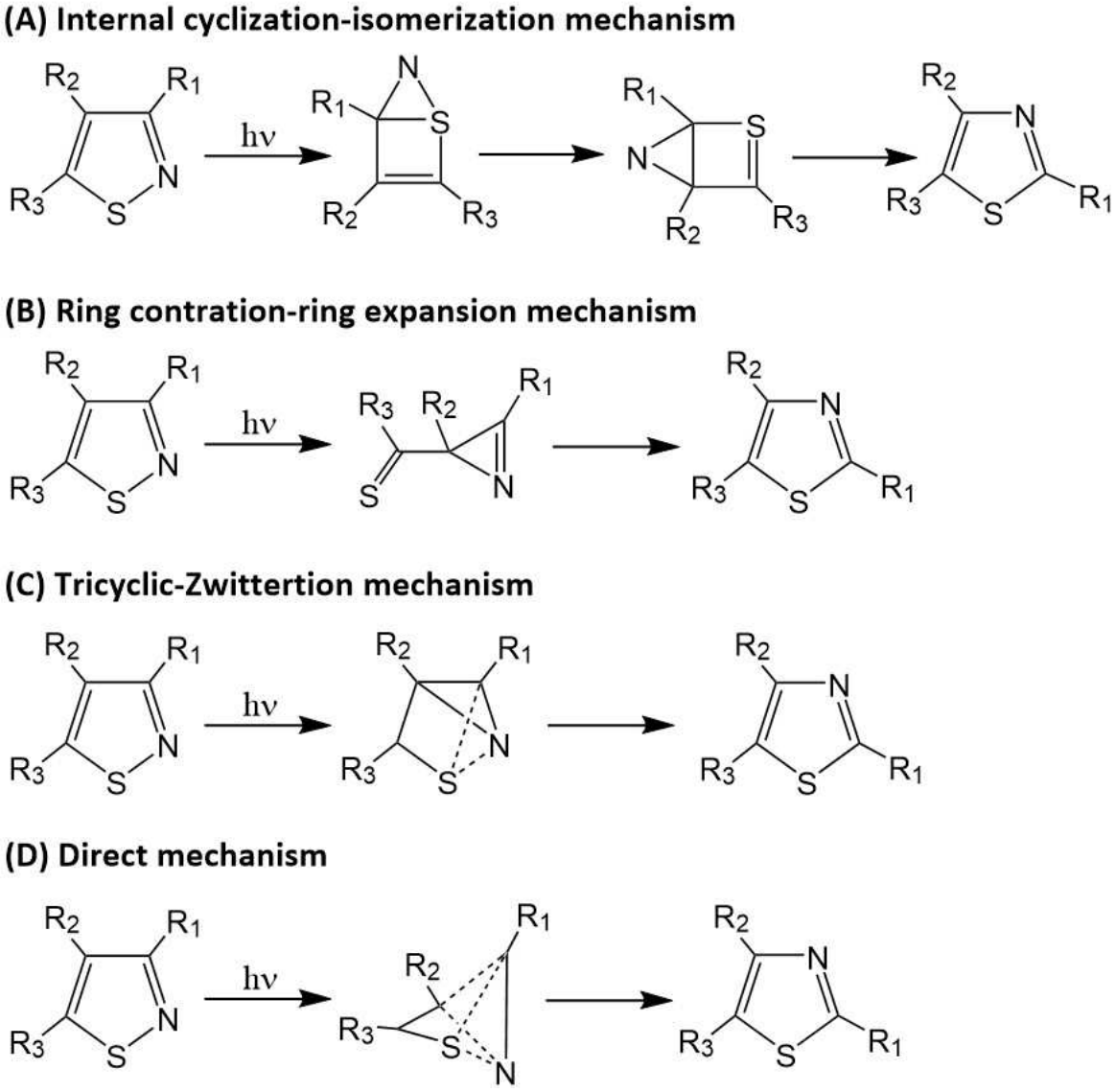

Scheme 2

Three mechanisms have been offered to rationalize the photorearrangement patterns of isothiazoles.[9] See Scheme 2. However, none of these proposed mechanisms can give a good explanation for the available experimental data[7,8] As a result, the mechanisms of isothiazole photo-transposition have not been understood.

It is these interesting experimental results and unsolved problems that inspire this study. To the best of the author's knowledge, no theoretical works have published photochemical mechanisms for isothiazoles. According to the available data,[7,8] it is thus suggested the fourth mechanism, the direct mechanism (Scheme 2(D)),[10] which can be used to rationalize the experimental results for the variously substituted isothiazoles mentioned.

In order to gain deeper insight into the phototransposition reaction mechanisms of 3–methylisothiazole (**Rea–1**), 4–methylisothiazole (**Rea–2**) and. 5–methylisothiazole (**Rea–3**), the CASSCF theory[10,11] was used to analyse their detailed potential energy surfaces. The reason for studying the photoisomerization reactions of methyl substituted isothiazoles is because they have already been experimentally studied (Scheme 1).[8] It is hoped that the present theoretical investigations, combined with previous experimental works,[7,8] will have a strong impact on the photorearrangement reactions of isothiazoles, since these photochemical rearrangement reactions should play a prominent role in determining the stereochemistry as well as the synthetic chemistry of a variety of photoreactions of isothiazoles.

II. Methodology

The CASSCF calculations were performed using the multiconfigurational self-consistent field (MCSCF) program released in Gaussian 09.[12] The active space used to describe the photoreactions of methylisothiazole and methylthiazole comprises ten electrons in seven orbitals, i.e., five p-π orbitals plus two nonbonding orbitals, located on a nitrogen and a sulfur atom. The CASSCF method was used with the 6-311G(d) basis sets for geometry optimization (vide

infra). The optimization of conical intersections was achieved in the (f – 2)-dimensional intersection space using the method of Bearpark et al.,[13] implemented in the Gaussian 09 program.[12] Unless otherwise noted, the relative energies given in the text are those determined at the MP2-CAS-(10,7)/6-311++G(3df,3pd) level using the CAS(10,7)/6-311G(d) (hereafter designed MP2-CAS[14] and CASSCF, respectively) geometry. The Cartesian coordinates and the energetics calculated for the various points, using both methods, is available as Supporting Information.

III. General Consideration

A general outline of the five π-p orbitals in unsubstituted isothiazole, which form the basis for this study, is shown in Scheme 3. The lowest singlet $\pi \rightarrow \pi^*$ excitation is the singlet π_3 (HOMO) $\rightarrow \pi_4^*$ (LUMO) transition. In the perturbed HOMO level, the electron density of the neighboring sulfur and nitrogen atoms is therefore increased (via the atomic orbital coefficients). Due to the reason that the π-electronic structures of methyl-substituted isothiazoles are analogous to those of unsubstituted isothiazole, their photo-excitations should be similar. For methylisothiazoles, Pavlik and co-workers also found no indication of the participation of a triplet state.[8] Triplet states thus play no role in the photoreactions studied herein.[15] Consequently, the photoisomerization reactions of methylisothiazoles must react on singlet surfaces and must also only involve the $\pi \rightarrow \pi^*$ transition. Therefore, it is focused on the singlet $^1(\pi, \pi^*)$ surfaces from now on.

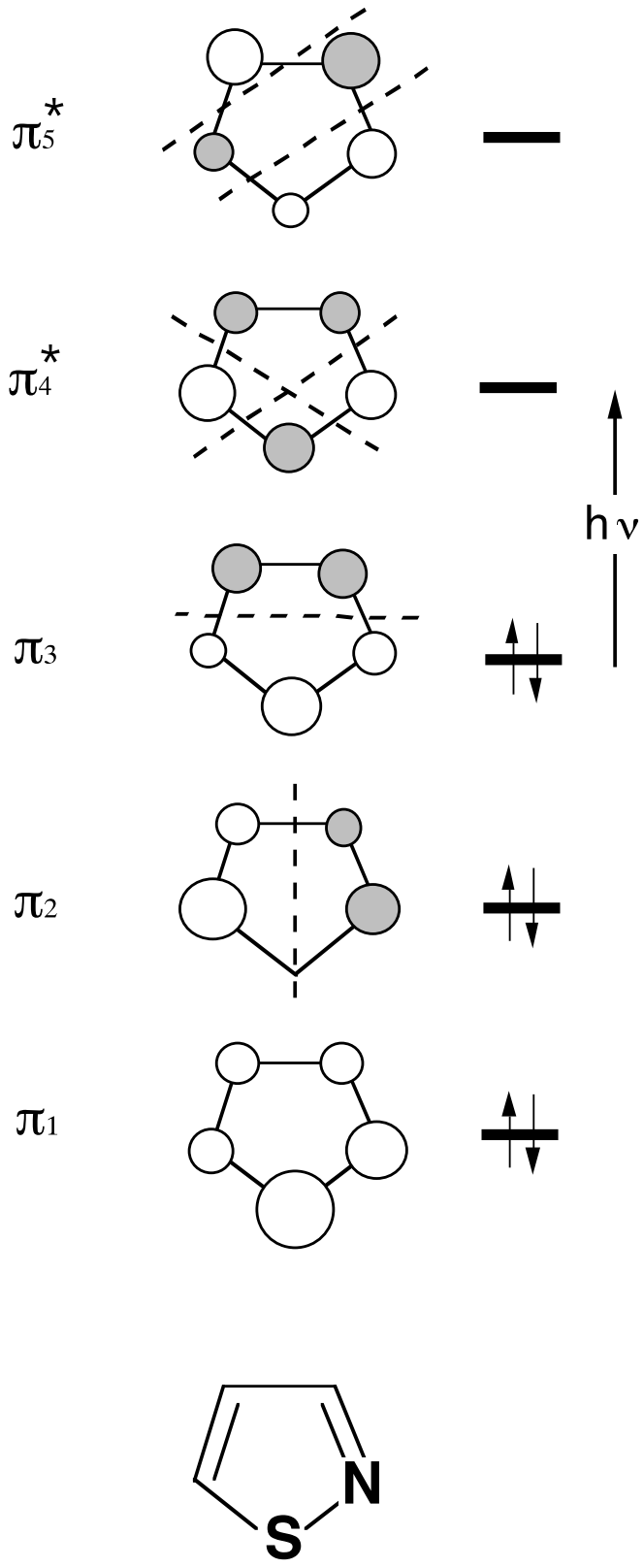

Scheme 3

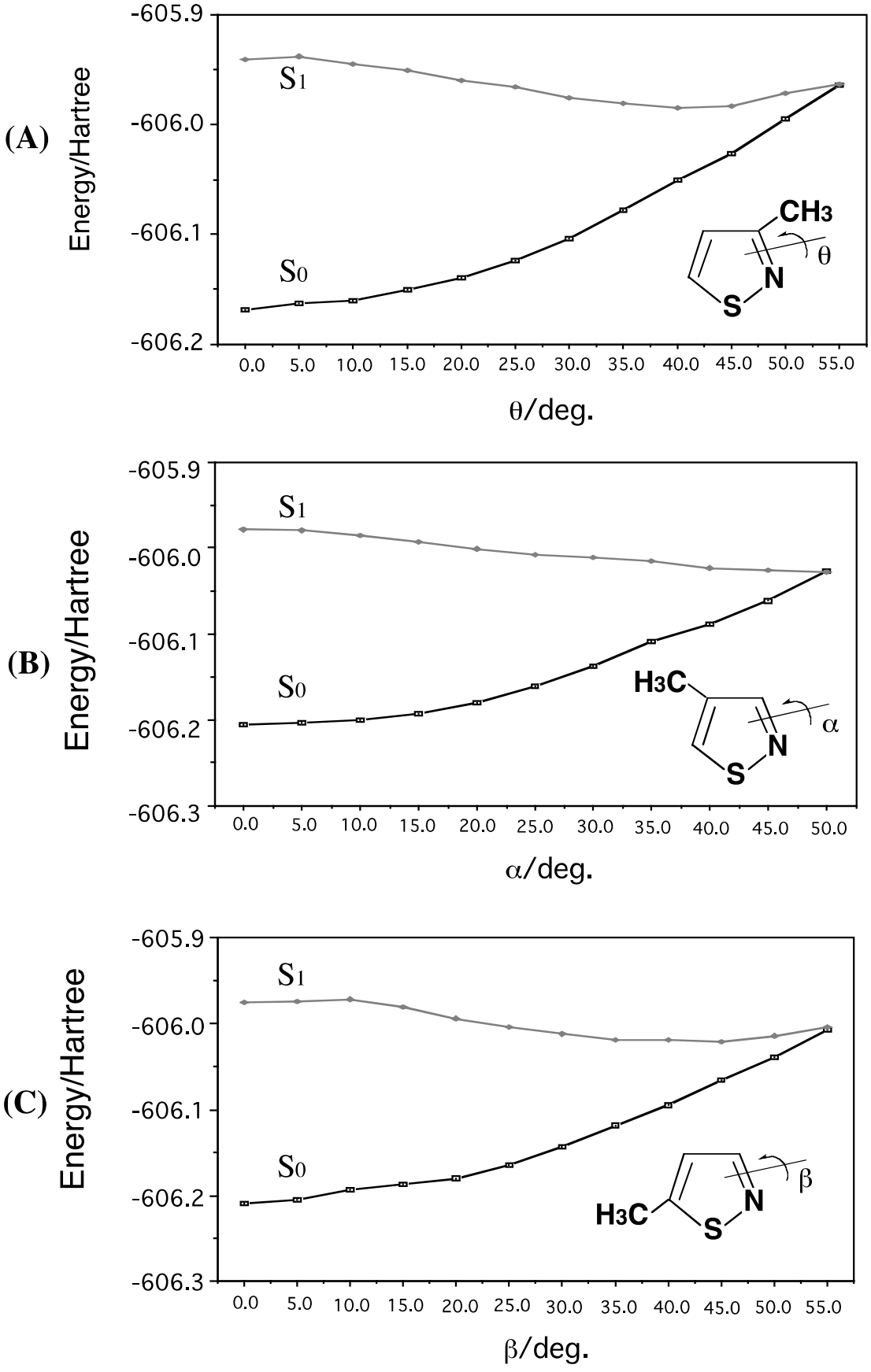

Figure 1: Three minimum-energy pathways of 3-methylisothiazole (A), 4-methylisothiazole (B), and 5-methylisothiazole (C) along the torsion angle coordinate optimized for the S_1 state at the CAS(10,7)/6-311G(d) level of theory.

The central part of the photochemical mechanisms of methylisothiazoles is the location of the conical intersection in the excited- and ground-electronic states. Figure 1(A) shows the qualitative potential energy surfaces for the S_0 and S_1 states of 3–methylisothiazole (**Rea–1**) as a function of rotation about the N_2=C_3 double bond (i.e., the rotation angle θ).[16,17] By twisting the N_2=C_3 π bond in **Rea–1**, the energy of both π_3 and π_4* increases, because there are increased antibonding interactions. Finally, these π orbitals become degenerate at a geometry of around 55° of rotation. The existence of a degenerate point, as a result of the rotation of the N_2=C_3 double bond, also strongly implies that there should be an inclined S_1/S_0 surface crossing at a very similar geometry. From there, decay to the ground state is fully efficient.[10] Again, for 4–methylisothiazole (**Rea–2**) and 5–methylisothiazole (**Rea–3**), twisting the N_2=C_3 π bonds can lead to degeneration of the S_0 and S_1 energy surfaces at about 50° and 55°, as shown in Figures 1(B) and 1(C), respectively.[16] These results are used to explain the mechanisms for the photochemical isomerization reactions of **Rea–1**, **Rea–2**, and **Rea–3** in the following section.

IV. Results and Discussion

(1) 3-Methylisothiazole

The photo-isomerization of 3-methylisothiazole (**Rea–1**) is firstly considered, as indicated in eq (1). From previous discussion, there are three possible types of reaction pathways on the singlet excited potential energy surface of **Rea–1**, all of which lead to the same photoproduct, 2-methylthiazole (**Pro–1**). Figure 2 represents all of the relative energies of the various points with respect to

the energy of the reactant, **Rea–1**. The structures of the various stationary points on the possible mechanistic pathways of Figure 2 are shown in Figures 3-5.

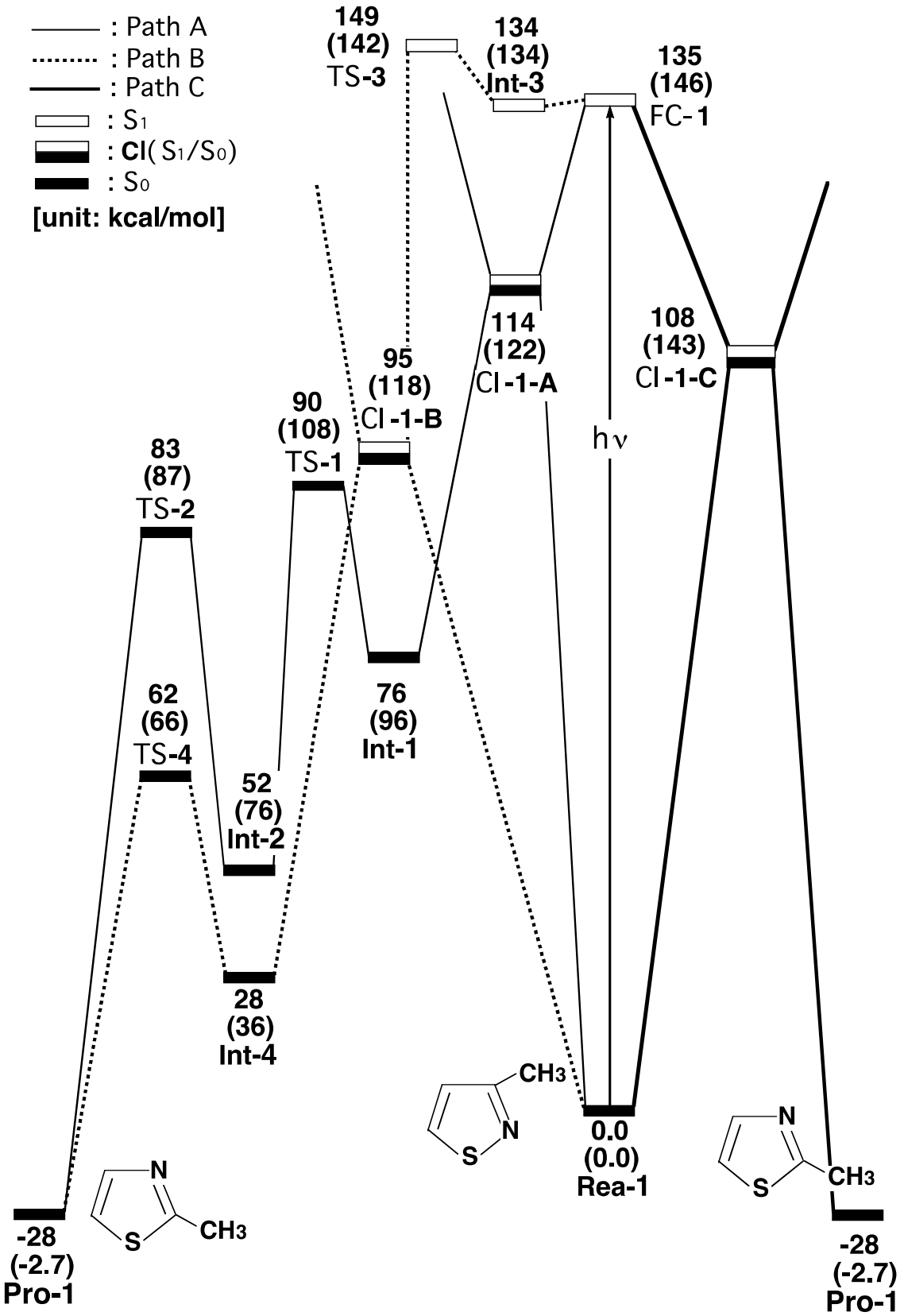

Figure 2: Energy profiles for the photoisomerization modes of 3-methylisothiazole (**Rea-1**). The abbreviations FC and CI stand for Frank–Condon and conical intersection, respectively. The relative energies were obtained at the CAS(10,7)/6-311G(d) (in parentheses) and MP2-CAS-(10,7)/6-311++G(3df,3pd)//CAS(10,7)/6-311G(d) levels of theory. All energies (in kcal/mol) are given with respect to the reactant (**Rea-1**). The CASSCF optimized structures of the crucial points see Figures 3-5. For more information see the text.

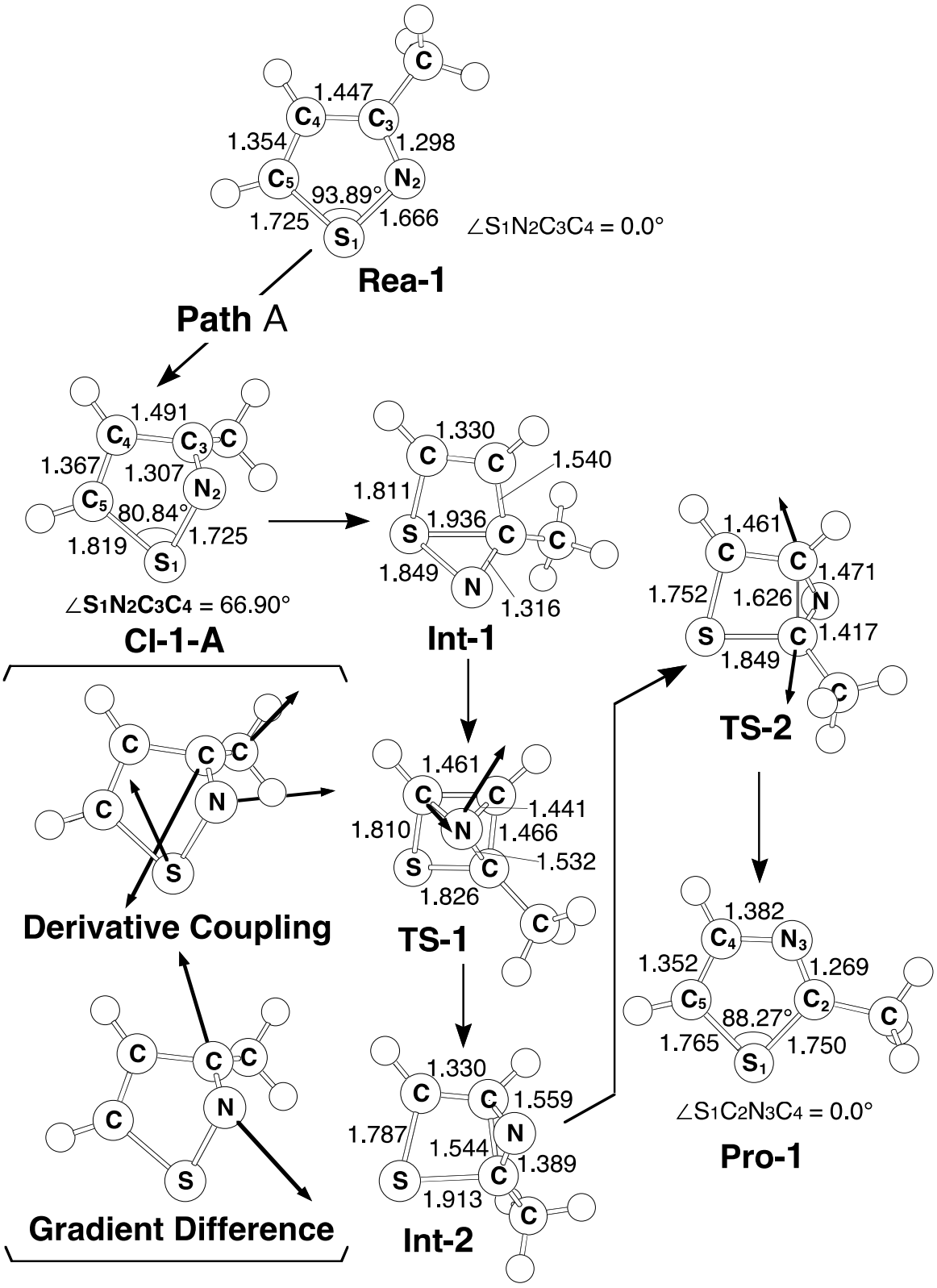

Figure 3: The CAS(10,7)/6-311G(d) geometries (in Å and deg) for path A of 3-methylisothiazole (**Rea-1**), conical

intersection (**CI**), intermediate, transition state (**TS**), and isomer products. The nonadiabatic coupling and gradient difference vectors—those which lift the degeneracy— computed with CASSCF at the conical intersections **CI-1-A**. The corresponding CASSCF vectors are shown inset. For more information see the Supporting Information.

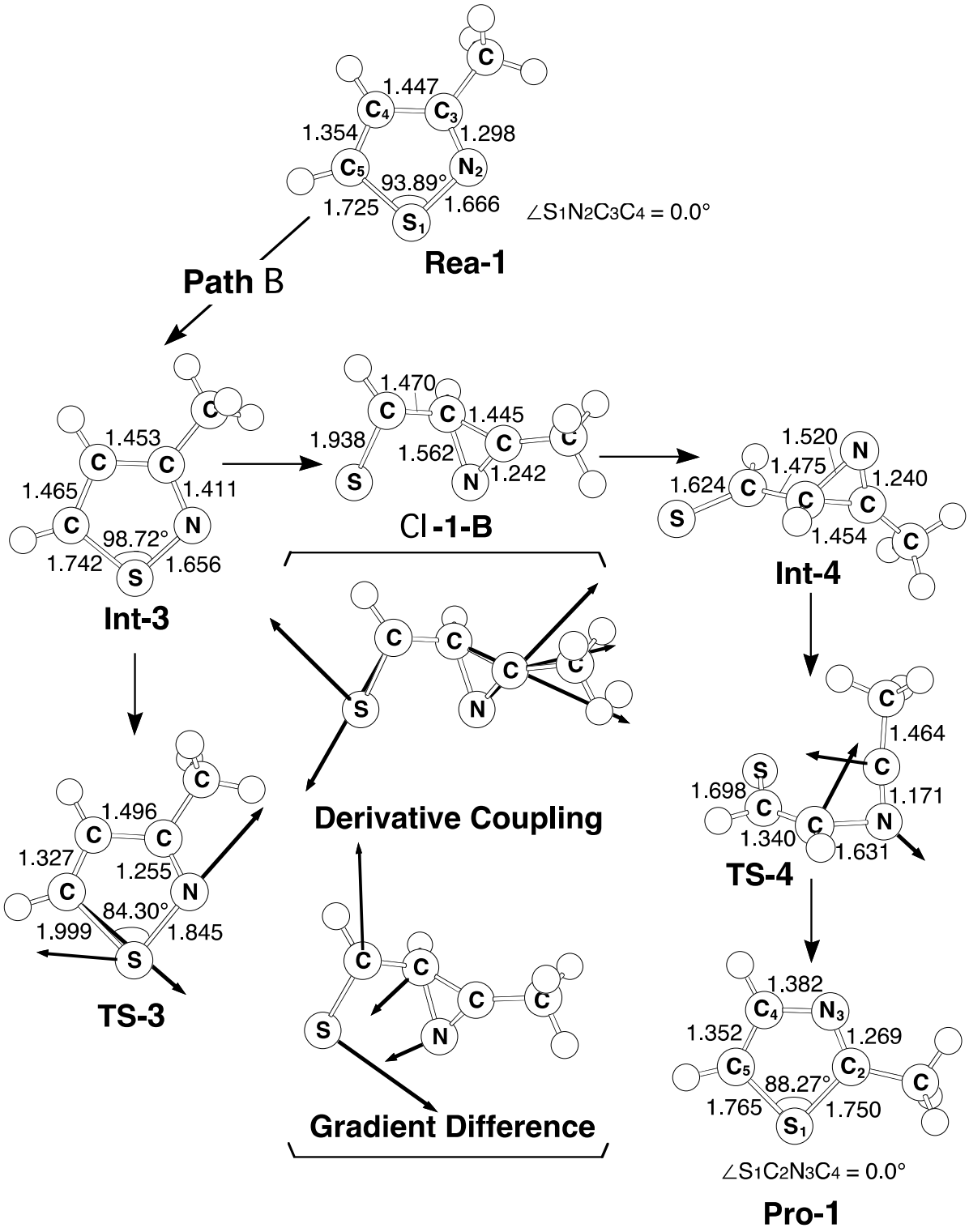

Figure 4: The CAS(10,7)/6-311G(d) geometries (in Å and deg) for path B of 3-methylisothiazole (**Rea-1**), conical intersection (**CI**), intermediate, transition state (**TS**), and isomer products. The nonadiabatic coupling and gradient

difference vectors—those which lift the degeneracy— computed with CASSCF at the conical intersections **CI-1-B**. The corresponding CASSCF vectors are shown inset. For more information see the Supporting Information.

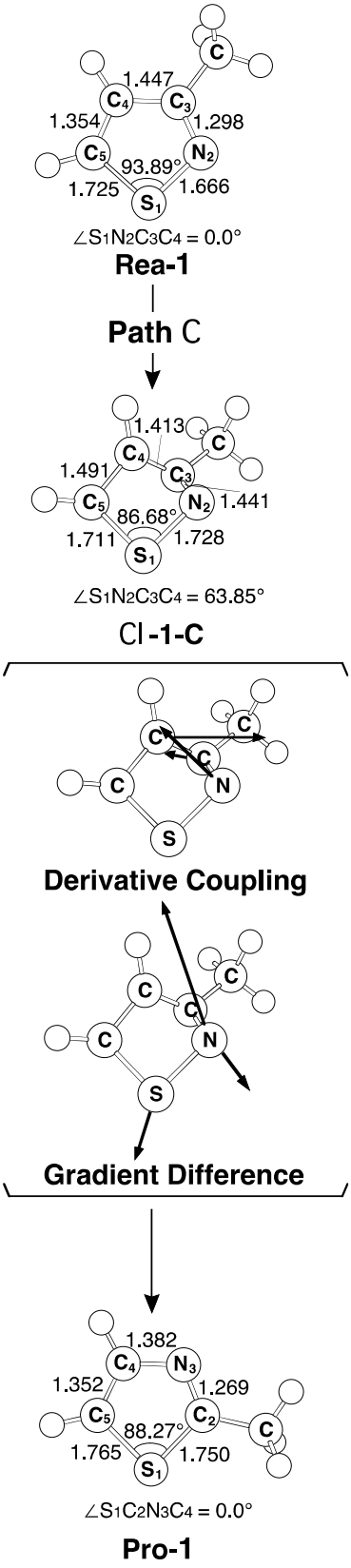

Figure 5: The CAS(10,7)/6-311G(d) geometries (in Å and deg) for path C of 3-methylisothiazole (**Rea-1**), conical

intersection (**CI**), intermediate, transition state (**TS**), and isomer products. The nonadiabatic coupling and gradient difference vectors—those which lift the degeneracy— computed with CASSCF at the conical intersections **CI-1-C**. The corresponding CASSCF vectors are shown inset. For more information see the Supporting Information.

In the first step, the reactant (**Rea–1**) is excited to its excited singlet state by a vertical excitation, as shown in the middle of Figure 2. The MP2-CAS vertical excitation energies to the lowest excited π* state of **Rea–1** is predicted to be 135 kcal/mol. As mentioned before, the calculated 135 kcal/mol band for **Rea–1** is best described as the $\pi_3 \rightarrow \pi_4^*$ transition.

Starting from the S_1 $^1(\pi_3 \rightarrow \pi_4^*)$ excited state of **Rea–1** results in S_1/S_0 **CI–1–A** (path A), **CI–1–B** (path B), or **CI–1–C** (path C). As shown in Figure 2, the theoretical results indicate that the energy of **CI–1–A** lies 114 kcal/mol above that of **Rea-1** and 21 kcal/mol lower in energy than that of **FC–1**. As seen in Figure 3, following the nonadiabatic coupling vector from S_1/S_0 **CI–1–A** (Figure 2) results in the formation of a bicyclic intermediate, **Int-1**, which is calculated to be 38 kcal/mol lower in energy than that of **CI–1–A**, but 76 kcal/mol higher than that of **Rea–1**. The next reaction step is a [1,3] shift of the nitrogen atom from C_3 to C_4, which happens through a transition state, **TS–1**. The barrier height at **TS–1**, measured from **Int–1**, is 19 kcal/mol. Thus, when **Int–2** is formed, four-membered ring opening by the C–C bond activation occurs via transition state **TS–2**, which is 21 kcal/mol above that of **Int–2**, and results in the final photoproduct **Pro–1**. Thus, the theoretical results indicate that the mechanism for path A proceeds as follows:

Path A: **Rea–1 → FC–1 → S_1/S_0 CI–1–A → Int–1 → TS–1 → Int–2 → TS–2 → Pro–1**.

For path B, from the Franck-Condon point (**FC–1**), **Rea–1** can relax to an excited state intermediate near the S_0 geometry. It is found that this local minimum of the singlet excited surface is denoted **Int–3** and is calculated to be 134 kcal/mol, which is slightly below the **FC–1** point, as illustrated in Figure 2. The MP2-CAS results predict that **TS–3** lies about 15 kcal/mol higher in energy than **Int–3**. This transition state, **TS–3**, can then go to another conical intersection **CI–1–B**. As shown in Figure 2, the MP2-CAS results suggest that **CI–1–B** is lower in energy than **TS–3** by 54 kcal/mol, but 95 kcal/mol above the corresponding reactant, **Rea–1**. By following the nonadiabatic coupling vector from **CI–1–B**, the system arrives at a three-membered intermediate, **Int–4**. On the basis of the MP2-CAS calculations, the relaxation energy from **CI–1–B** to **Int–4** is estimated to be 67 kcal/mol. As seen in Figure 4, **TS–4** adopts a structure in which the formation of one bond between the S atom and the C atom produces the new five-membered ring product, **Pro–1**. The computed barrier at the transition state **TS–4** from the local minimum **Int–4** is 34 kcal/mol, at the MP2-CAS level of theory. Moreover, this value is much smaller than the energy (67 kcal/mol) from **CI–1–B** to **Int–4**. In consequence, once the **CI–1–B** is formed, the reactant can readily produce the photoproduct, **Pro–1**, through the **Int–4** → **TS–4** process. Therefore, the process for path B is represented as follows:

Path B: **Rea–1** → **FC–1** → **Int–3** → **TS–3** → **S_1/S_0 CI–1–B** → **Int–4** → **TS–4** → **Pro–1**.

The computational results demonstrate that the path C channel is an one–step process, which only involves the S_1/S_0 **CI–1–C** point. Namely, starting from the **FC–1** point, 2- **Rea–1** enters an extremely efficient decay channel, S_1/S_0

CI–1–C. From this point, the photo-isomer **Pro–1** and the initial reactant **Rea–1** are reached via a barrier-less ground-state relaxation pathway. Accordingly, the process for path C is described as follows:

Path C: **Rea–1** → **FC–1** → **S_1/S_0 CI–1–C** → **Pro–1**.

(2) 4-Methylisothiazole

The photo-isomerization of 4-methylisothiazole (**Rea–2**), as indicated in eq (2), is then considered. In this section, the three reaction routes for **Rea–2** are compared (Scheme 2). The entire potential energy surface is collected in Figure 6. The structures of the various stationary points on the mechanistic pathways of Figure 6 are shown in Figures 7-9.

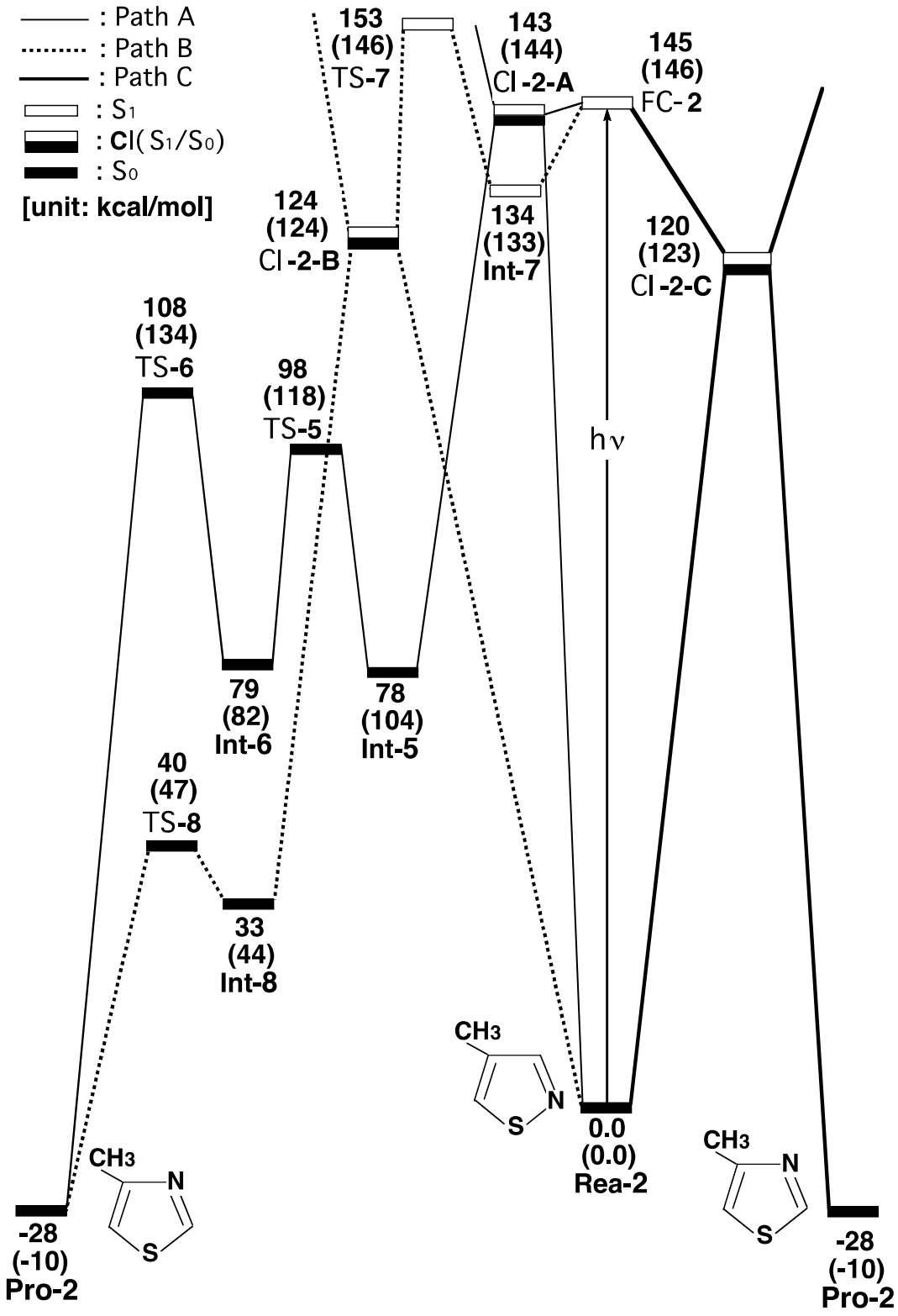

Figure 6: Energy profiles for the photoisomerization modes of 4-methylisothiazole (**Rea-2**). The abbreviations FC and CI stand for Frank–Condon and conical intersection, respectively. The relative energies were obtained at the CAS(10,7)/6-311G(d) and MP2-CAS-(10,7)/6-311++G(3df,3pd)//CAS(10,7)/6-311G(d) and (in parentheses) levels of theory. All energies (in kcal/mol) are given with respect to the reactant (**Rea-2**). The CASSCF optimized structures of the crucial points see Figures 7-9. For more information see the text.

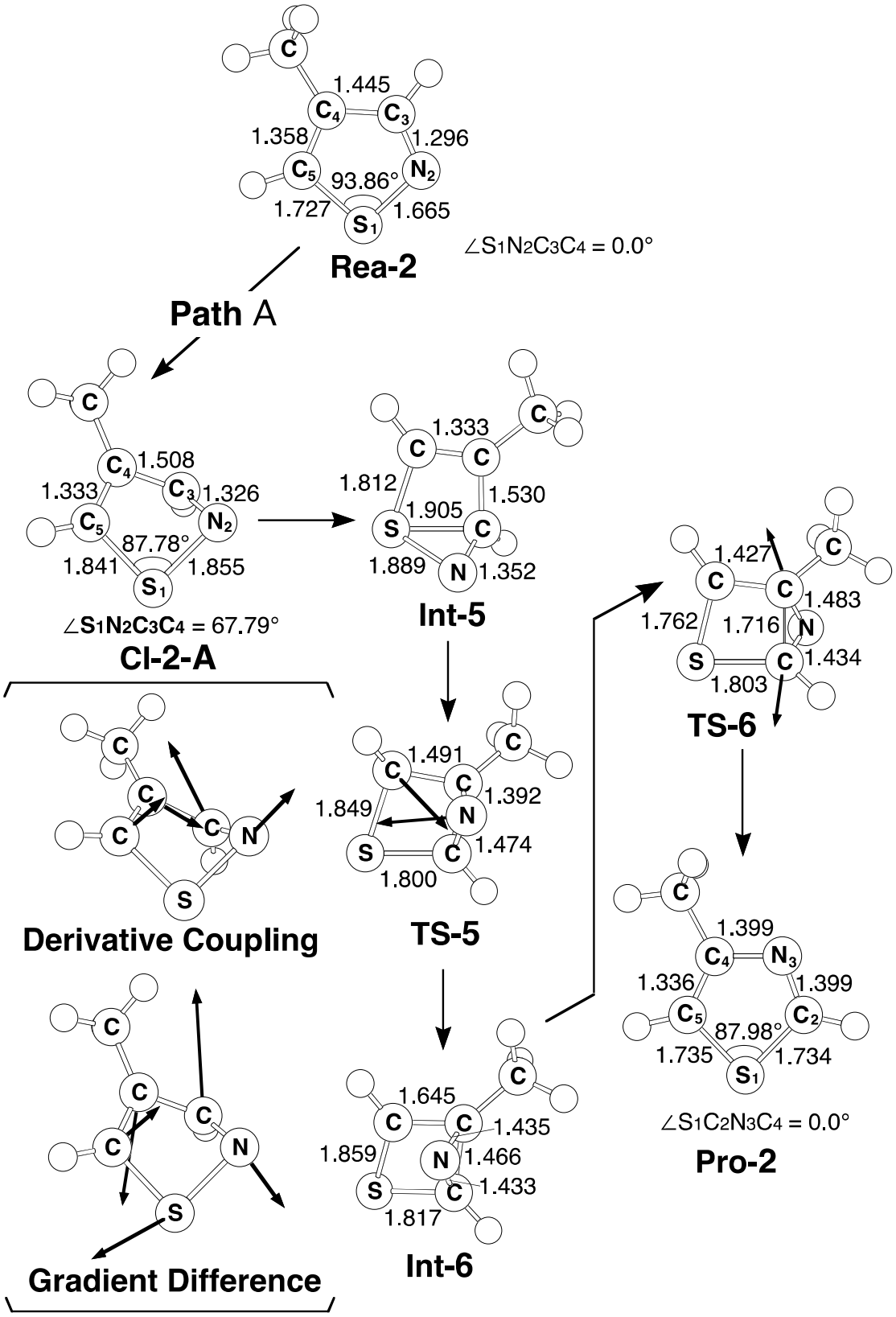

Figure 7: The CAS(10,7)/6-311G(d) geometries (in Å and deg) for path A of 4-methylisothiazole (**Rea-2**), conical intersection (**CI**), intermediate, transition state (**TS**), and isomer products. The nonadiabatic coupling and gradient difference vectors—those which lift the degeneracy— computed with CASSCF at the conical intersections **CI-2-A**. The corresponding CASSCF vectors are shown inset. For more information see the Supporting Information.

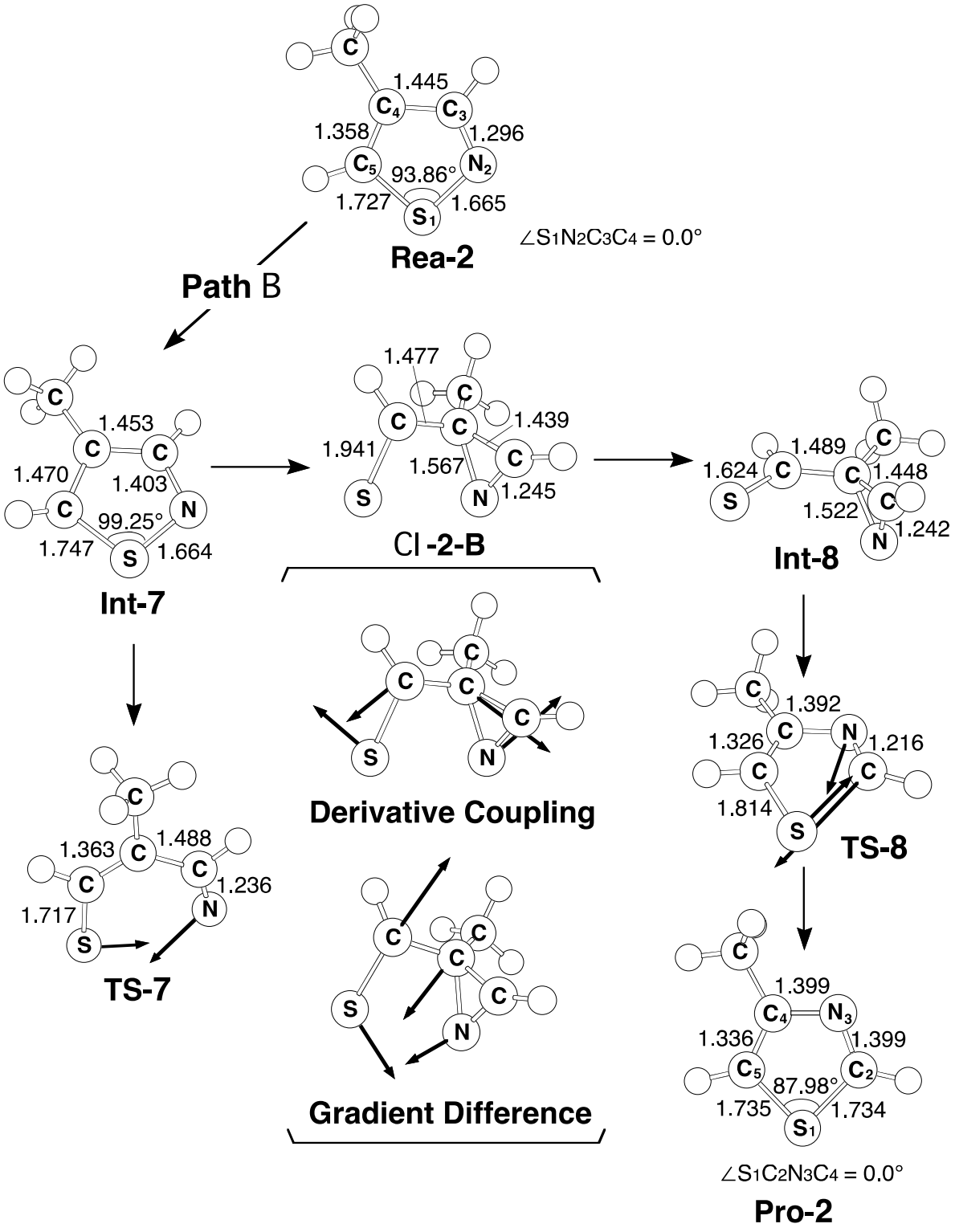

Figure 8: The CAS(10,7)/6-311G(d) geometries (in Å and deg) for path B of 4-methylisothiazole (**Rea-2**), conical intersection (**CI**), intermediate, transition state (**TS**), and isomer products. The nonadiabatic coupling and gradient difference vectors—those which lift the degeneracy— computed with CASSCF at the conical intersections **CI-2-B**. The corresponding CASSCF vectors are shown inset. For more information see the Supporting Information.

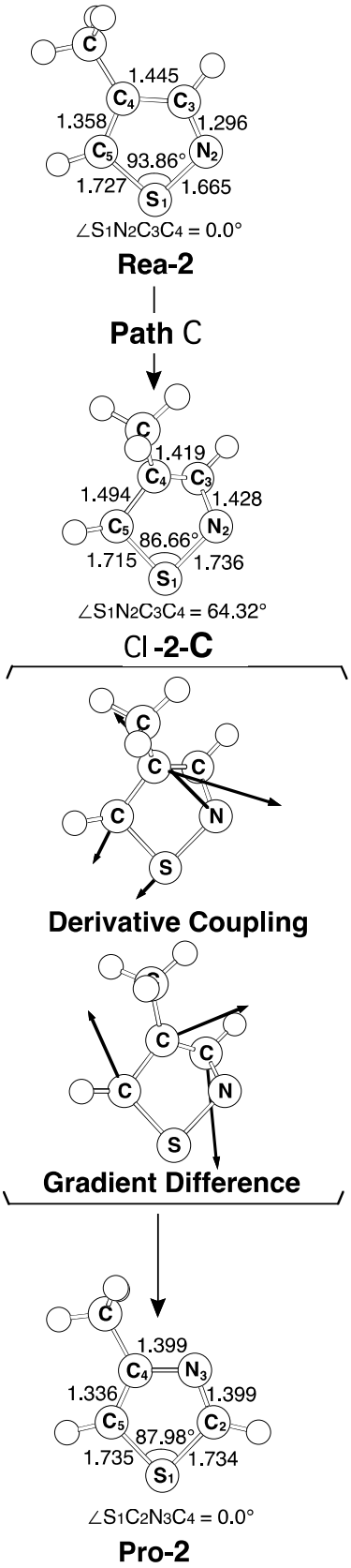

Figure 9: The CAS(10,7)/6-311G(d) geometries (in Å and deg) for path C of 4-methylisothiazole (**Rea-2**), conical intersection (**CI**), intermediate, transition state (**TS**), and isomer products. The nonadiabatic coupling and gradient difference vectors—those which lift the degeneracy— computed with CASSCF at the conical intersections **CI-2-C**. The corresponding CASSCF vectors are shown inset. For more information see the Supporting Information.

The MP2-CAS vertical excitation energy to the lowest excited π* state of **Rea–2** (**FC–2**) is estimated to be 145 kcal/mol. As seen in Figure 7, by following the gradient difference vector from **CI–2–A**, the system arrives at a bicyclic local intermediate, **Int–5**. The next reaction step on path A is the shift of the nitrogen atom, which results in another bicyclic minimum, **Int–6**, via **TS–6**. The MP2-CAS calculations indicate that the process of bicyclic ring formation from **Int–5** to give **Int–6** is almost thermally neutral (Figure 6) and has an activation barrier of 20 kcal/mol. When **Int–6** has been formed, the C_4–C_5 bond activation can occur via the transition state **TS–7**, which is 29 kcal/mol above **Int–6**. Accordingly, the model results suggest that, once the conical intersection **CI–2–A** is produced, the reactant molecule (**Rea–2**) reaches the final photoproduct, **Pro–2,** without any difficulty. The theoretical observations thus reveal that path A for **Rea–2** proceeds as follows:

Path A: **Rea–2** → **FC–2** → **S_1/S_0 CI–2–A** → **Int–5** → **TS–6** → **Int–6** → **TS–7** → **Pro–2**.

The first step in path B for **Rea–2** is the formation of a local minimum **Int–7** on the singlet excited state ($\pi_3 \rightarrow \pi_4^*$). The transition state, **TS–8**, which connects **Int–7** and **CI–2–B**, is given in Figure 8. The energy of **TS–8** is computed to be 19 kcal/mol higher than the excited state **Int–7**. After decay at the conical intersection **CI–2–B**, the local minimum, **Int–8**, and the initial reactant, **Rea–2**, are reached via a barrier-less ground-state relaxation pathway. The theoretical results estimate that the energy of **CI–2–B** is greater than that of **Rea–2** and **Int–8** by 124 and 91 kcal/mol, respectively, but lower than that of **FC–2** by 10 kcal/mol. Overcoming this barrier leads to the final photoproduct,

Pro–2, which has an exothermic enthalpy of 28 kcal/mol. As a result, the theoretical study reveals that the photoisomerization reaction in path B proceeds as follows:

Path B: **Rea–2** → **FC–2** → **Int–7** → **TS–8** → **S_1/S_0 CI–2–B** → **Int–8** → **TS–9** → **Pro–2**.

Finally, the path C channel is an one–step process, which only contains a S_1/S_0 **CI–2–C** point. The MP2-CAS results estimate that S_1/S_0 **CI–2–C** is lower than **FC–2** by 25 kcal/mol in energy and the competing S_1/S_0 **CI–2–A** and **CI–2–B** are higher in energy than S_1/S_0 **CI–1–C** by 23 and 4.0 kcal/mol, respectively. In consequence, the process for path C is described as follows:

Path C: **Rea–2** → **FC–2** → **S_1/S_0 CI–2–C** → **Pro–2**.

(3) 5-Methylisothiazole

Finally the photo-rearrangement of 5-methylisothiazole (**Rea–3**), as stated in eq (3), is considered. Similarly to the cases of **Rea–1** and **Rea–2**, the photorearrangement reactions of **Rea–3** studied in the present work potentially follow similar reaction paths to those discussed previously. The potential energy profiles for the photo-rearrangements of **Rea–3** at the MP2-CAS and CASSCF levels are represented in Figure 10. The structures of the various stationary points on the mechanistic pathways of Figure 10 are shown in Figures 11-13.

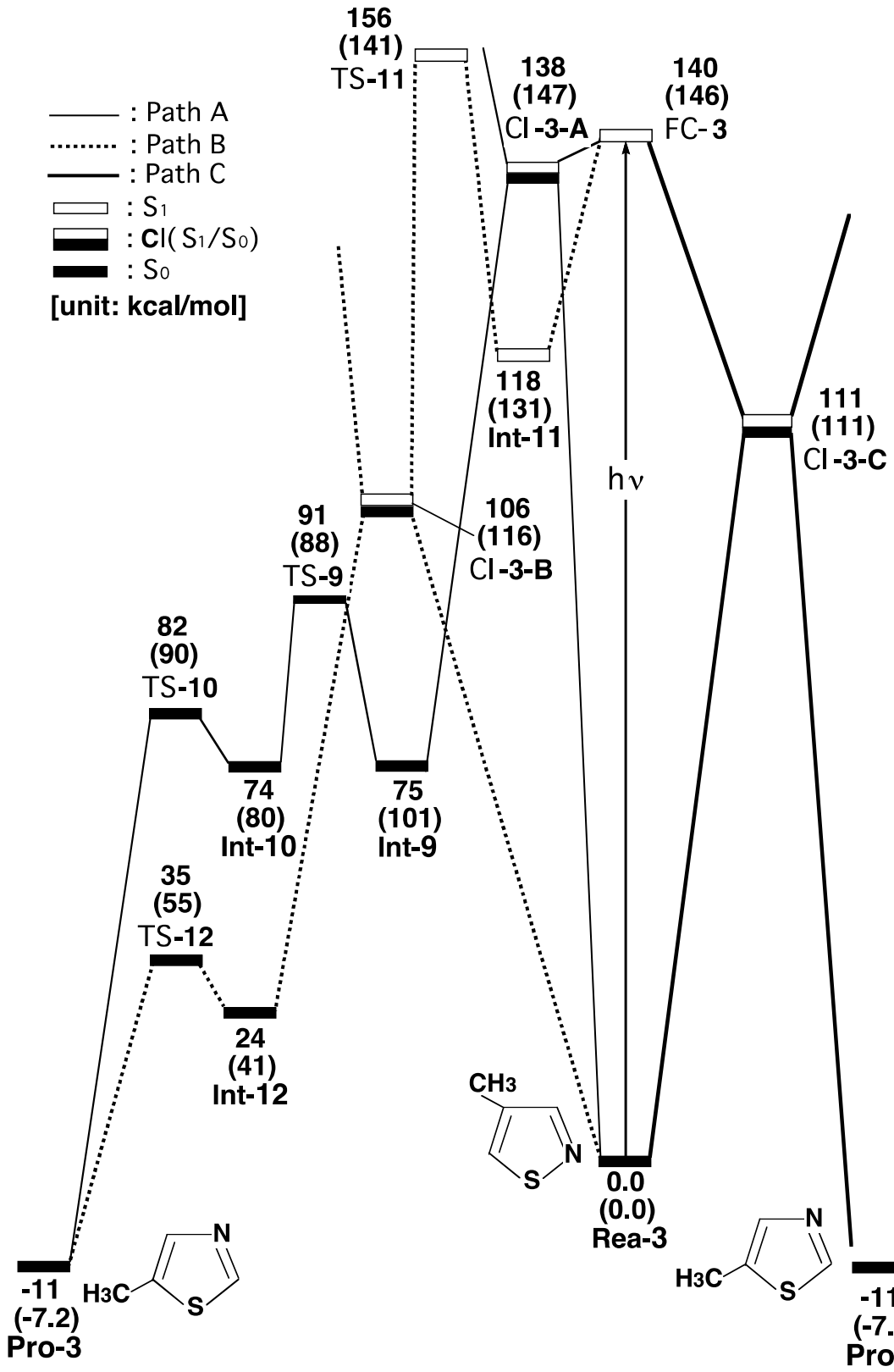

Figure 10: Energy profiles for the photoisomerization modes of 5-methylisothiazole (**Rea-3**). The abbreviations FC and CI stand for Frank–Condon and conical intersection, respectively. The relative energies were obtained at the CAS(10,7)/6-311G(d) and MP2-CAS-(10,7)/6-311++G(3df,3pd)//CAS(10,7)/6-311G(d) and (in parentheses) levels of theory. All energies (in kcal/mol) are given with respect to the reactant (**Rea-3**). The CASSCF optimized structures of the crucial points see Figures 11-13. For more information see the text.

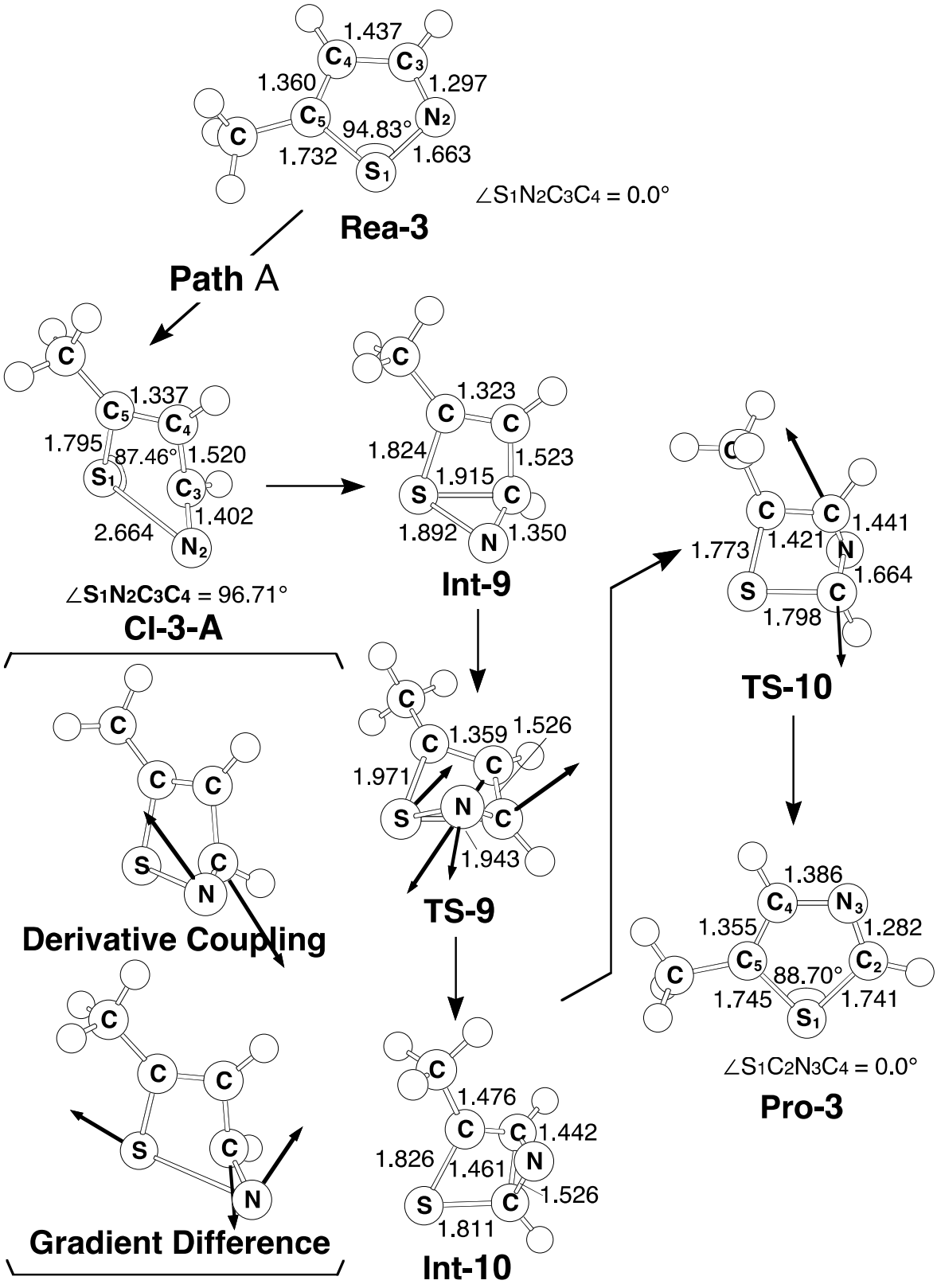

Figure 11: The CAS(10,7)/6-311G(d) geometries (in Å and deg) for path A of 5-methylisothiazole (**Rea-3**), conical intersection (**CI**), intermediate, transition state (**TS**), and isomer products. The nonadiabatic coupling and gradient difference vectors—those which lift the degeneracy— computed with CASSCF at the conical intersections **CI-3-A**. The corresponding CASSCF vectors are shown inset. For more information see the Supporting Information.

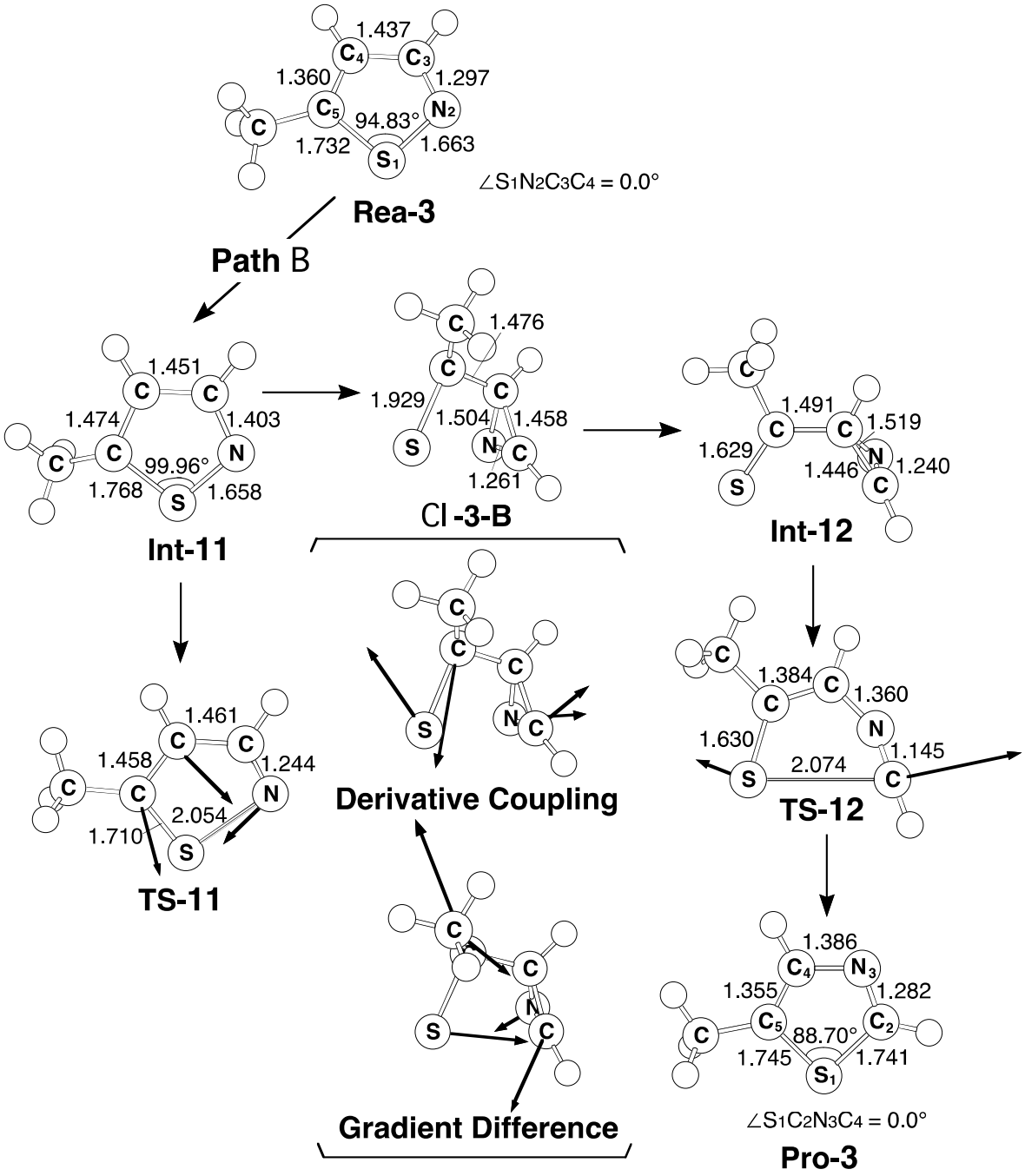

Figure 12: The CAS(10,7)/6-311G(d) geometries (in Å and deg) for path B of 5-methylisothiazole (**Rea-3**), conical intersection (**CI**), intermediate, transition state (**TS**), and isomer products. The nonadiabatic coupling and gradient difference vectors—those which lift the degeneracy— computed with CASSCF at the conical intersections **CI-3-B**. The corresponding CASSCF vectors are shown inset. For more information see the Supporting Information.

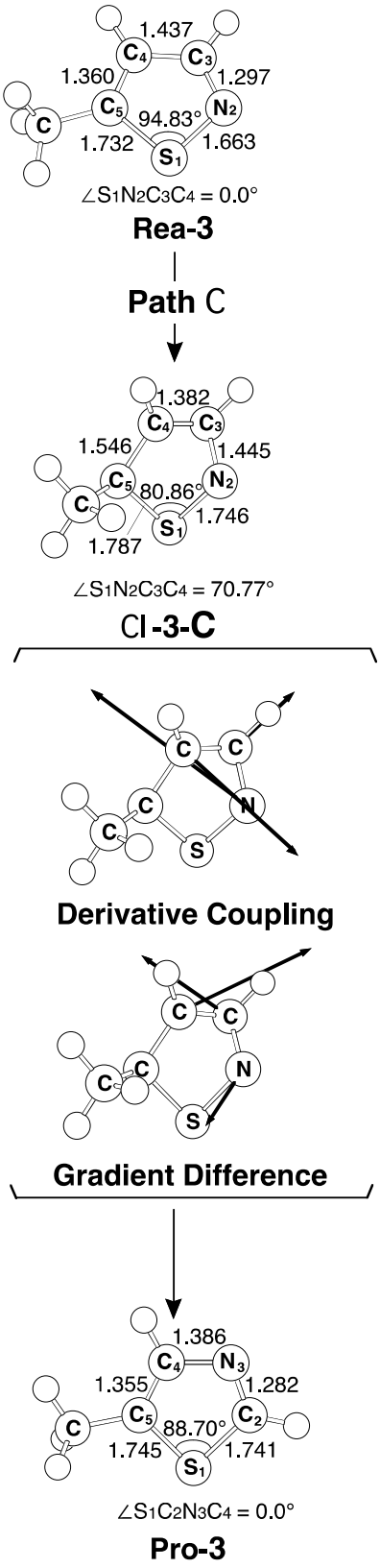

Figure 13: The CAS(10,7)/6-311G(d) geometries (in Å and deg) for path C of 5-methylisothiazole (**Rea-3**), conical intersection (**CI**), intermediate, transition state (**TS**), and isomer products. The nonadiabatic coupling and gradient difference vectors—those which lift the degeneracy— computed with CASSCF at the conical intersections **CI-3-C**. The corresponding CASSCF vectors are shown inset. For more information see the Supporting Information.

The geometry optimizations result in three conical intersections (i.e., **CI–3–A**, **CI–3–B** and **CI–3–C**), which are respectively 2.0, 34 and 29 kcal/mol lower in energy than **FC–3**. The [1,3] shift of the N atom into another bicyclic minimum proceeds through **TS–9**. The computational results predict that the energy of **Int–10** is lower than that of the **TS–9** species by 17 kcal/mol. From **Int–10**, C–C bond breaking (i.e., via **TS–10**) occurs and conventional formation of a five-membered ring occurs, with activation energy of 8.0 kcal/mol. It is noteworthy that the **Rea–3** molecule has an overall energy of more than 60 kcal/mol, which is much larger than the energy difference between **Int–9** and **TS–9** (16 kcal/mol) and that between **Int–10** and **TS–10** (8.0 kcal/mol). As a result, these two barriers can be easily surmounted. The MP2-CAS calculations also demonstrate that the final photoproduct, **Pro–3**, is exothermic by 11 kcal/mol. Consequently, the mechanism for path A is represented as follows:

Path A: **Rea–3** → **FC–3** → **S_1/S_0 CI–3–A** → **Int–9** → **TS–11** → **Int–10** → **TS–12** → **Pro–3**.

The first step for **Rea–3** in path B is the formation of a minimum, **Int–11**, with a relieved energy of 22 kcal/mol, at the MP2-CAS level of theory. As seen in Figure 10, the next forward reaction is: **TS–11** → **S_1/S_0 CI–3–B** → **Int–12** → **TS–12** → **Pro–3**. However, the MP2-CAS results reveal that the barrier height from **Int–11** to **TS–11** (38.0 kcal/mol) is higher than the energy difference between **FC–3** and **Int–11** (32.0 kcal/mol). This information strongly indicates that it is unlikely that the **Rea–3** molecule follows the mechanism of path B (i.e., the ring contraction–ring expansion pathway). The mechanism for the singlet photoisomerization of **Rea–3** in path B is given below.

Path B: **Rea–3** → **FC–3** → **S_1/S_0 CI–3–B** → **Int–12** → **TS–14** → **Pro–3**.

Finally, once the $S_0 \rightarrow S_1$ vertical excitation occurs, the system relaxes from the **FC–3** point to the conical intersection **CI–3–C**, which is 29 kcal/mol lower in energy. In fact, by following the nonadiabatic coupling vector from **CI–3–C** and rotating an N_2–C_3 bond, the system arrives at a photoproduct with a methyl group ring on position 5, **Pro–3**. In consequence, the process for path C is as follows:

Path C: **Rea–3** → **FC–3** → **S_1/S_0 CI–3–C** → **Pro–3**.

V. Conclusion

The photochemical reaction mechanisms of various substituted isothiazoles, are studied with respect to permutation of the ring atoms. Three types of substituted isothiazoles (**Rea-1**, **Rea-2**, and **Rea-3**) are chosen. Taking all of the systems studied in this paper together, the following conclusions can be drawn:

(1) From the present study, if a heterocyclic molecule that has the N and S atoms, which can absorb a photon to arrive at an excited singlet state, via a $^1(\pi \rightarrow \pi^*)$ transition, then this molecule rotates a heterocyclic ring bond. This excited molecule can thus enter an extremely efficient decay channel, a conical intersection point between the excited- and ground-state potential energy surfaces. After decay at this point, the molecule continues its evolution on the ground state potential surface to produce various products.[10,11]

(2) An internal cyclization–isomerization pathway (path A), a ring contraction–ring expansion pathway (path B) and a direct pathway (path C), are used to described the photorearrangements of methyl substituted isothiazoles. The

model results suggest that path C is more favorable than either path A or path B, from both energetic and kinetic viewpoints, regardless of the position at which the methyl substituent is attached to the isothiazole molecule.

It is hoped that the present work can stimulate further research into this subject.

Acknowledgments

The author is grateful to the National Center for High-Performance Computing of Taiwan for generous amounts of computing time, and the National Science Council of Taiwan for the financial support. The author also wishes to thank Professor Michael A. Robb, Dr. S. Wilsey, Dr. Michael J. Bearpark, (University of London, UK) and Professor Massimo Olivucci (Universita degli Studi di Siena, Italy), for their encouragement and support during his stay in London. Special thanks are also due to reviewers 1 and 2 for very help suggestions and comments.

References:

(1) For reviews, see: (a) Wooldridge, K. R. H. *Adv. Heferocycl. Chem.* **1972**, *14*, 1. (b) Kurzer, F. *Organic Compounds of Sulphur, Selenium, and Tellurium*, Vol. I, The Chemical Society, London, 1970, pp 369-377. (c) Kurzer, F. *ibid.* **1973**, *11*, 556. (d) Barton, D.; Ollis, W. D. *Comprehensive Organic Chemistry, The Synthesis and Reactions of Organic Compounds*; Pergamon Press: NewYork, 1979; vol. 4, Heterocyclic Compounds. (e) Pain, D. L.; Peart, B. J.; Wooldridge, K. R. H. *Comprehensive Heterocyclic Chemistry,* vol. 6, ed. Potts, K. T.; Katritzky, A. R.; Rees, C. W. Pergamon, Oxford, **1984**, ch. 4.17, p. 131. (f) Chapman, R. F.; Peart, B. J. *Comprehensive Heterocyclic Chemistry II, vol. 3*, ed. Shinkai, I.; Katritzky, A. R.; Rees, C. W.; Scriven, E. F. V. Pergamon, Oxford, 1996, ch. 3.05, p. 319. (g) Kaberdin, R. V.; Potkin, V. I. *Russ. Chem. Rev.* **2002**, *71*, 673. (h) Brown, D. W.; Sainsbury, M. *Science of Synthesis.* vol. 11, ed. Schaumann, E., 2002, p. 567. (i) Elgazwy, A.-S. S. H. *Tetrahedron*. **2003**, *59*, 7445.

(2) Lawson, A.; Tinkler, R. B. *Chem. Rev.* **1970**, *70*, 593.

(3) Larson, E. R.; Noe, M. C.; Gant , T. G. *US Pat.* 6 235 764, 2001.

(4) Slack, R.; Wooldridge, K. R. H. *Adv. Heterocycl. Chem.* **1965**, *4*, 107.

(5) Davis, M. *Adv. Heterocycl. Chem.* **1972**, *14*, 43.

(6) For instance, see: Potts, K. T. *Comprehensive Heterocyclic Chemistry, The Structure, Reactions, Synthesis and Uses of Heterocyclic Compounds*, ed. Katritzky, A. R. and Rees, C. W., Pergamon Press, Oxford, 1984, vol. 6

(7) (a) Wynberg, H.; van Driel, H.; Kellogg, R. M.; Buter, J. *J. Am. Chem. Soc.* **1967**, *89*, 3487. (b) Catteau, J. P.; LaBlache-Combier, A.; Pollet, A. *J. Chem. Soc., Chem. Commun.* **1969**, 1018. (c) Lablache-Combier, A.; Pollet, A. *Tetrahedron* **1972**, *28*, 3141.

(8) Pavlik, Pavlik, J. W.; Pandit, C. R.; Samuel, C. J.; Day, A. C. *J. Org. Chem.* **1993**, *58*, 3407.

(9) For instance see: (a) Padwa, *A. Rearrangements in Ground and Excited States*; de Mayo, P., Ed.; Academic Press: New York, 1980; Vol. 3, p 501 ff.

Lablache-Combier, (b) A. *Photochemistry of Heterocyclic Compounds; Burchard,* O., Ed.; Wiley-Interscience: New York, 1976; Vol. 4, p 123 ff.

(10) For excellent reviews, see: (a) F. Bernardi, M. Olivucci, M. A. Robb, *Isr. J. Chem.* **1993**, 265. (b) M. Klessinger, *Angew. Chem. Int. Ed. Engl*. **1995**, *34*, 549. (c) F. Bernardi, M. Olivucci, M. A. Robb, *Chem. Soc. Rev*. **1996**, 321. (d) F. Bernardi, M. Olivucci, M. A. Robb, *J. Photochem. Photobio. A: Chem.* **1997**, *105*, 365. (e) M. Klessinger, *Pure Appl. Chem.* **1997**, *69*, 773. (f) M. Klessinger, J. Michl In *Excited States and Photochemistry of Organic Molecules,* VCH Publishers, New York, 1995.

(11) (a) Olivucci, M.; Ragazos, I. N.; Bernardi, F.; Robb, M. A. *J. Am. Chem. Soc.* **1993**, *115*, 3710. (b) Bernardi, F.; Olivucci, M.; Ragazos, I. N.; Robb, M. A. *J. Am. Chem. Soc.* **1992**, *114*, 8211.

(12) M. J. Frisch, et al. Gaussian, Inc., Wallingford CT, 2010.

(13) Bearpark, M. J.; Robb, M. A.; Schlegel, H. B. *Chem. Phys. Lett*. **1994**, *223*, 269.

(14) McDouall, J. J. W.; Peasley, K.; Robb, M. A. *Chem. Phys. Lett*. **1988**, *148*, 183.

(15) Nevertheless, the CASSCF results indicate that the energetics of triplet states for **Rea-1**, **Rea-2**, and **Rea-3** are higher than the corresponding ground singlet isomers by 33, 37, and 31, respectively.

(16) The bond lengths in the 5-membered-ring, S–N, N–C, S–C, C–C, and C–H bonds of isothiazole are fixed to be 1.30, 1.30, 1.30, 1.30, and 1.09 Å, respectively. Also, the bond angles in the 5-membered-ring ∠CSN, ∠SNC, ∠NCC, and ∠CCC are fixed to be 108°, 108°, and 108°, respectively.

(17) 1 eV = 23.119 kcal/mol.

TOC